Mini review

Electrochemiluminescent Biosensors for the Detection of MicroRNAs: A Review

Linlin Hou[1,]and Binbin Zhou[1,2,*]*

[1] Henan Province of Key Laboratory of New Optoelectronic Functional Materials, College of Chemistry and Chemical Engineering, Anyang Normal University, Anyang, Henan 455000, People's Republic of China
[2] Hunan Institute of Food Quanlity Supervision Inspection and Research, Building B, No. 238, Ave. Timesun, District Yuhua, Changsha, Hunan 410111, People's Republic of China
[*]E-mail: linlin9918@163.com, bbzhou1985@163.com

MicroRNAs have been regarded as the new markers for cancer diagnosis and treatment. Electrochemiluminescence (ECL) with the merits of electrochemistry and chemiluminescence exhibits high sensitivity, low background, fast response and high simplicity. This work focused on the recent progress in the design strategies for miRNAs detection with ECL biosensors.

1. INTRODUCTION

MicroRNAs (miRNAs) are a class of 21 ~ 25mer long non-protein-coding small RNAs found in eukaryotes. They can degrade or inhibit the translation of target gene through complete or incomplete matching with target gene 3'UTR, thus accurately regulating the development, differentiation, proliferation, apoptosis and immune regulation of organisms [1]. Recently, abnormal expression of miRNAs has been found in a variety of tumors, which is closely related to the progress, clinical treatment and prognosisb of tumors [2, 3]. Therefore, miRNAs are becoming the new targets for cancer diagnosis and treatment [4-6]. At present, simple and sensitive methods for miRNAs detection are still highly desired. Electrochemiluminescence (ECL) is a phenomenon of luminescence caused by the electron transfer of reactants on the surface of electrodes and the accompanying chemical reactions. It combines the advantages of electrochemical and chemiluminescent methods [7, 8]. ECL does not require to introduce external light sources. Compared with photoluminescence, ECL

can effectively avoid the interference of background light sources and improve signal-to-noise ratio. In contrast to chemiluminescence, ECL can only produce luminescence under electrochemical excitation. This method exhibits high sensitivity, low background, fast response and high simplicity. ECL has been widely used in bio-immunoassay, medical diagnosis, food and environmental monitoring, and has become one of the important methods for in vitro diagnosis [7, 9]. Recently, we and other groups have addressed the progress in the electrochemical and optical detection of miRNAs [1, 10-13]. However, to the best of our knowledge, there is no specific review paper focusing on the progress in design strategies for miRNAs detection with ECL biosensors. In this review, we summarized the development of ECL miRNAs biosensors in recent five years (2014 - 2018).

2. STRATEGIES FOR ECL BIOSENSORS

2.1. Hemin

To date, the H_2O_2/luminol ECL system is still one of the most popular systems. To improve the ECL emission of this system, electrochemically catalytic reactions by nanomaterials have been widely employed to enhance the efficiency. Hemin with mimicking peroxidase activity can promote the decomposition of H_2O_2 and the generation of reactive oxygen species (ROS) by intercalating into the dsDNA grooves. With hemin as the ECL reporter, the ECL signal can be enhanced in the H_2O_2/luminol system. For example, Chai's group reported an ECL biosensors for miRAN-155 detection based on the signal amplification of hybridization chain reaction (HCR) and hemin mimicking peroxidase [14]. Target miRAN-155 triggered the formation of dsDNA polymers on electrode surface via the HCR, thus allowing for the intercalation of a large number of hemin and amplifying the ECL signal. Furthermore, Chai's group reported a novel structure for miRNA detection, namely a "K" type bonding structure consisting of a substrate DNA and a reporter DNA [15]. The target miRNA can simultaneously be hybridized with the five prime end of substrate DNA and the three prime of the reporter DNA to form a double strand. The fragment of the substrate DNA that hybridizes with the miRNA can be decomposed by the lambda exonuclease (λ-exo). The fragment that is not digested in the substitute DNA becomes the trigger DNA. At the same time, miRNAs were released to participate in the next cycle. The trigger DNA and miRNA led to the formation of the "K" structure which can be linearly and exponentially decomposed, respectively. Finally, only the single strand reporter DNA remained on the electrode for hemin-binding through the formation of hemin/G-quadruplex complexes. Recently, Lu and co-workers reported an ECL method for miRNA detection with the signal amplification of glucose oxidase (GOD) and hemin [16]. The AuNPs-modified electrode was covered with capture probe DNA for hybridization with the target miRNA and blocked with GOD for catalyzing the oxidation of glucose to produce H_2O_2. Hemin acts as a catalyst to catalyze the generation of ROS by decomposing the produced H_2O_2, thereby enhancing the ECL signal after reaction with luminol.

2.2. Ru Complexes

The Ru complexes exhibit high ECL efficiency, good biocompatibility and stability. Besides H_2O_2/luminol system, Ru complexes-based system is also one of the most popular ECL systems [17]. For example, Xu and Yang first developed a miRNA ECL biosensor by intercalating $Ru(phen)_3^{2+}$ into the dsDNA duplexes with the signal amplification of HCR in 2014 [18]. The $Ru(phen)_3^{2+}$ attached on the electrode surface enhanced the ECL signal. Moreover, an effective co-reactant can improve the ECL intensity and the detection sensitivity of bioassays in the Ru complexes-based systems.[19] For example, tripropylamine (TPrA) can be commonly used as co-reagent to enhance the ECL signal of Ru complexes [20]. Yin's group reported an ECL biosensor for miRNA319a detection by the signal amplification of two-stage isothermal chain displacement polymerase reaction [21]. The target miRNA hybridized with the part of DNA template to form a double strand, and then the other part of DNA template without participating in the hybridization forms a double strand by replication with the help of Phi29 polymerase. Nt.BsmAI, a nicking endonuclease, recognizes the junction site of template DNA and target miRNA, thereby resulting in the cleavage of the hybrid DNA strand and the release of a single strand DNA. The released DNA is continuously produced in the presence of Phi29 polymerase and Nt.BsmAI. This is the first isothermal chain displacement polymerase reaction. Next, the loop portion of a hairpin probe DNA modified by Ru/TPrA compound on electrode surface was hybridized with the released DNA, thus resulting in the quenching of ECL signal. At the same time, the primer fragment can hybridize to the portion of the probe, thereby opening the loop of the hairpin probe. Since the Ru/TPrA structure is far from the GO electrode, the ECL signal is enhanced.

2.3. Metal nanomaterials

Since the discovery of ECL resonance energy transfer (RET) in 2009, the RET-based ECL quenching mechanism has been employed as a strategy for enhancing the sensitivity of biosensors. The systems have included metal nanomaterials (NPs) and nanoclusters (NCs), quantum dots and carbon nanomaterials [22, 23]. The progress in designing of miRNAs biosensors with the RET-based ECL systems has been addressed herein.

2.3.1 Ag NCs

Noble metal nanoclusters such as Au NCs and Ag NCs show low toxicity, good biocompatibility and excellent stability [24, 25]. With Ag NCs as signal markers, Xu's group first reported an ECL method for miRNA detection by RET effect (Figure 1) [26]. The target miRNA as a linker allowed for the capture of DNA-encapsulated Ag NCs by hybridization with the molecular beacon on electrode surface. Because the ECL spectrum of CdS NCs is close to that of Ag NCs and CdS NCs can be reduced by Ag NCs, the ECL signal of CdS NCs was quenched by the closed Ag NCs in the presence of co-reactant $K_2S_2O_8$. Additionally, Yuan's group reported the detection of miRNA by the signal amplification of target-cycling (TR) and rolling circle amplification (RCA) (Figure 2) [27]. The primers were modified on electrode surface for capture of a circular DNA template with many

guanine groups and hybridization with the target miRNA. Specifically, in the presence of miRNA, the primer formed a "P" linkage structure with circular DNA. In the presence of Phi29 DNA polymerase, more cytosine-rich fragments can be produced by RCA amplification. As a result, the Ag NCs can be formed by electrochemical reduction of Ag^+ with cytosine-rich fragment as template. The Ag NCs produced a strong ECL signal due to the RET-based ECL effect. In the process, the target miRNA was released to solution, thus allowing the next round of hybridization.
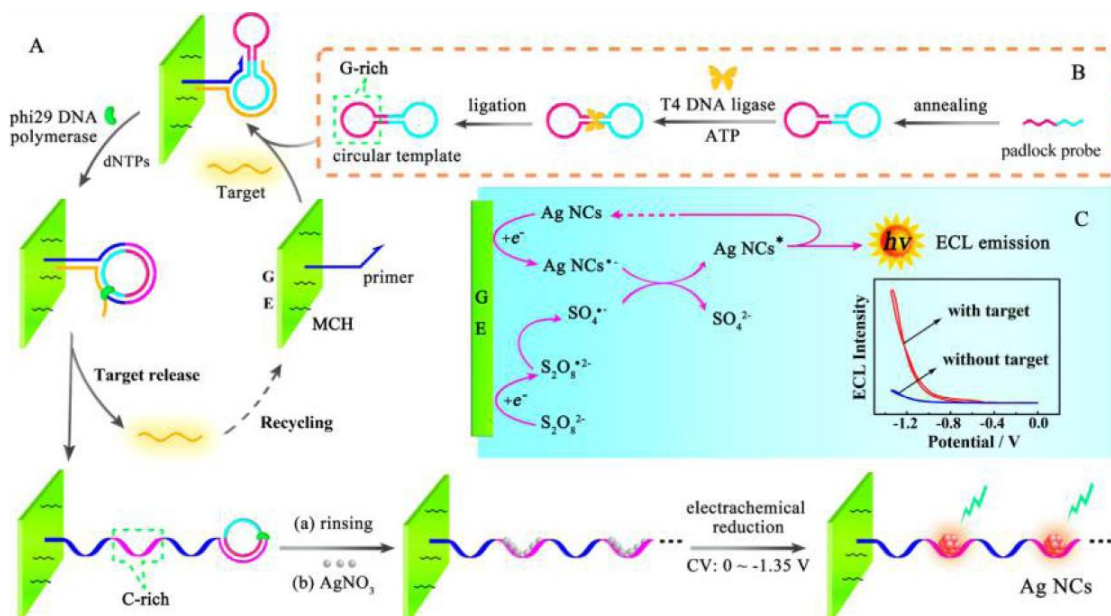
Figure 1. Schematic illustration of (A) the principle of target-cycling synchronized RCA and in situ electrochemical generation of Ag NCs, (B) preparation of the circular template, and (C) ECL mechanism of Ag NCs/$S_2O_8^{2-}$-based ECL system. Reprinted with permission from reference [26]. Copyright 2015 American Chemical Society.
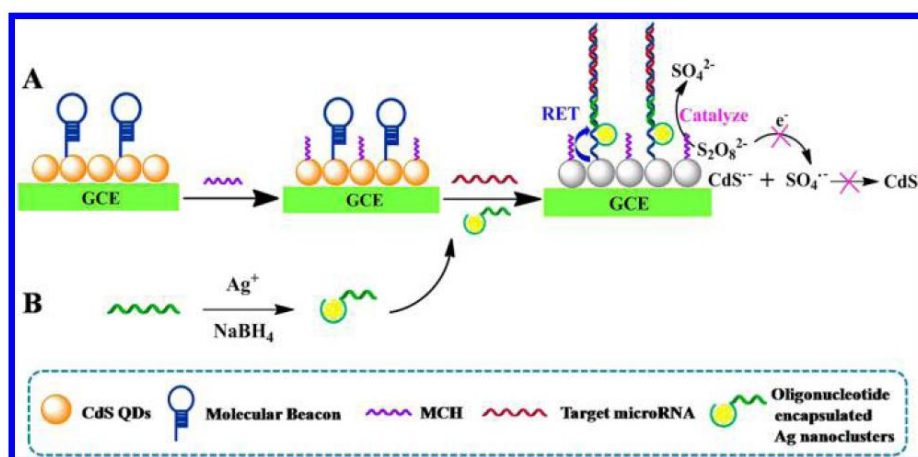
Figure 2. (A) Quenched ECL for detection of miRNA using oligonucleotide encapsulated Ag nanoclusters based on ECL RET and electron transfer and (B) synthesis of oligonucleotide encapsulated Ag nanoclusters. Reprinted with permission from reference [27]. Copyright 2016 American Chemical Society.

2.3.2 Au nanomaterials

Gold nanoparticles (AuNPs) can facilitate the electron transfer of redox reporters and enhance the loading of signal/capture probes because of their high conductivity and large surface area [28, 29]. Yuan's group reported a bi-directional DNA walking machine for ECL "off-on" detection of miRNA with AuNPs as the quenchers [30]. As shown in Figure 3, the DNA tracks consisting of three prominent chains of T1, T2 and T3 are immobilized on the surface of CdS:Mn nanocrystal electrode. The DNA walker is composed of two single chains (W1, W2), wherein AuNPs are modified with W2. A2 is a ssDNA that can hybridize with T2 and W1, and D1 is a ssDNA that can hybridize with the target miRNA21 to make it detached from the electrode. In the presence of the target miRNA-21, W2-capped AuNPs can be captured by the hybridization between miRNA-21 and W2 as well as T1. With the addition of A2 and D1, the target miRNA21 would be released and W2-capped AuNPs would be removed to close the electrode surface. This induced the decrease in the ECL signal due to the RET effect between AuNPs and CdS:Mn nanocrystals. However, addition of miRNA-155 led to the walking of W2-capped AuNPs from the electrode, increasing the distance between AuNPs and CdS:Mn nanocrystals and resulting in the recovery of the ECL signal. Therefore, the sensing electrode can be used to detect two different miRNAs. At the same time, Yuan's group reported a 3D DNA walking machine for ECL detection of miRNA (Figure 4) [31]. The AuNPs are modified on the magnetic Fe_3O_4 sphere. Then the walker, protecting and supporting DNA probes were immobilized on the AuNPs to form a 3D DNA walking machine. Target miRNAs can hybridize with the protecting DNA, allowing for the walker DNA to be released and hybridized with the supporting DNA. Next, the walker DNA was cleaved by Nt.BsmAI to release the intermediate DNA. The released intermediate DNA can hybridize with signal probe DNA S2 on AuNPs surface to open the hairpin structure of S2. This increased the distance between AuNPs and CdS: Mn QDs, thus resulting in the recovery of the ECL signal.
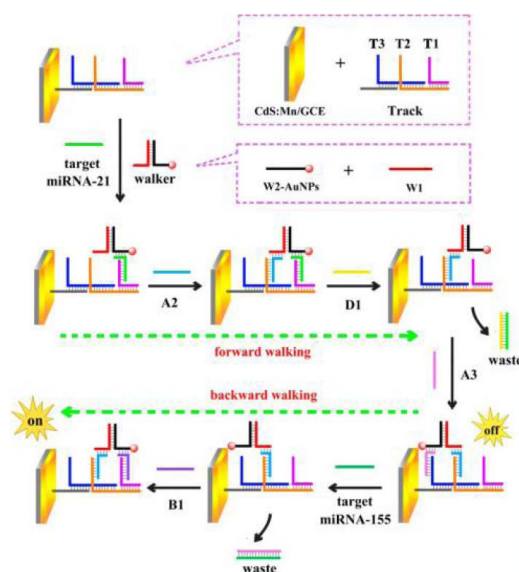
Figure 3. Schematic illustration of the miRNAs induced bidirectional DNA walking machine for sensitive detection of miRNAs. Reprinted with permission from reference [30]. Copyright 2017 American Chemical Society.
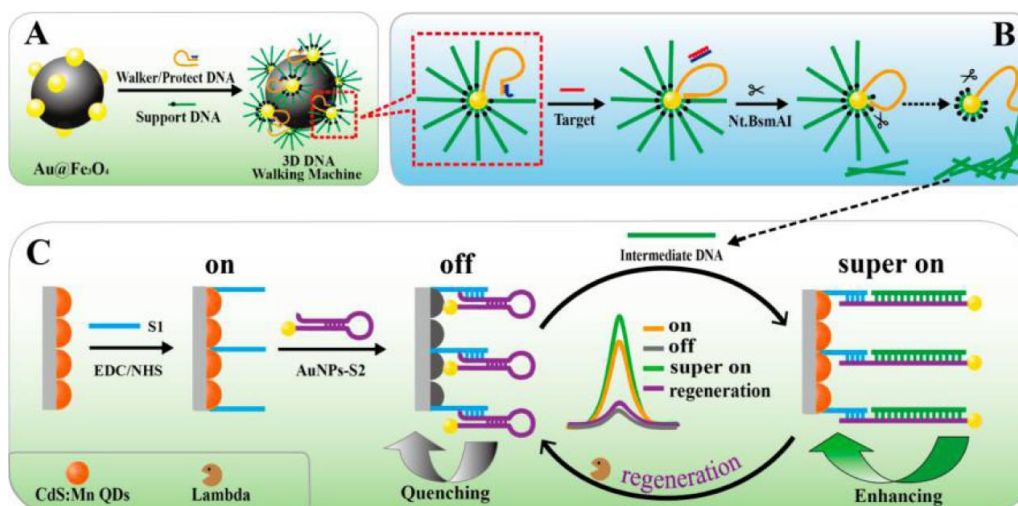
Figure 4. Preparation process of the 3D DNA walking machine (A), principles of the 3D DNA walking machine for target conversion (B), and schematic diagram of the "on−off−super on" ECL biosensor (C). Reprinted with permission from reference [31]. Copyright 2017 American Chemical Society.

Moreover, Guo and Zheng demonstrated that the signal ECL intensity of luminol can be enhanced by modifying the reaction microenvironment [32]. As shown in Figure 6, Hydrophobic microporous channel can be formed on the surface of bare gold electrode by using the self-assembly of 1,6-hexanedithiol. Luminol molecules can be immobilized on the microporous channel to produce an ECL signal that is three times higher than that on the unmodified electrode. The modified electrode can be used to detect miRNA with the aid of AuNPs. Without the target miRNA, the ssDNA probes were adsorbed onto the surface of AuNPs, thus preventing the adsorption of AuNPs on the electrode surface. However, the formation of ssDNA/miRNA duplex led to the increase of free AuNPs, thus facilitating the attachment of AuNPs on the electrode surface. In the latter, a poor ECL signal was achieved because of the closing gate effect and the quenching effect of AuNPs.
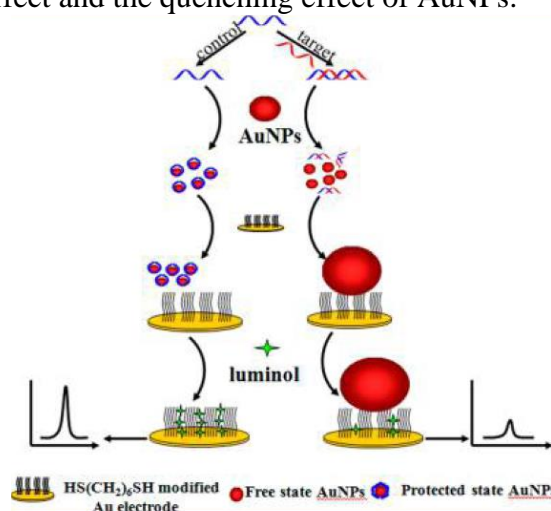
Figure 5. Cartoon representation of the proposed method for ECL detection of miRNA. Reprinted with permission from reference [32]. Copyright 2018 American Chemical Society.

A sensing interface was applied to ECL detection of microRNA in Zheng's group [23]. The interface was generated by target-guided assembly of AuNPs on an electrode modified with Nafion, carbon nanotubes and polyvinylpyrrolidone. The AuNPs acted as signal transduction probes and luminol used as the ECL reagent. The ss-DNA-capped AuNPs was formed when ss-DNA probes and AuNPs are present. In this case, the capped-AuNP did not assemble at the interface of the modified electrode and resulted in the ECL weaken because of the poor electroconductivity of PVP. However, if ss-DNA probes bound to target miRNA, the AuNPs can't interact with the DNA/miRNA hybrids. Therefore, AuNPs were aggregated and concentrated at the surface of the modified GCE and electrocatalyzed the oxidation of luminol to produce a strong ECL signal. The calibration plot is linear in the range of 40 fM to 1 pM with a detection limit of 20 fM. The method had been applied to discriminate most let-7 miRNA family members. The results demonstrated this sensing interface on clinically relevant cancer biomarkers.
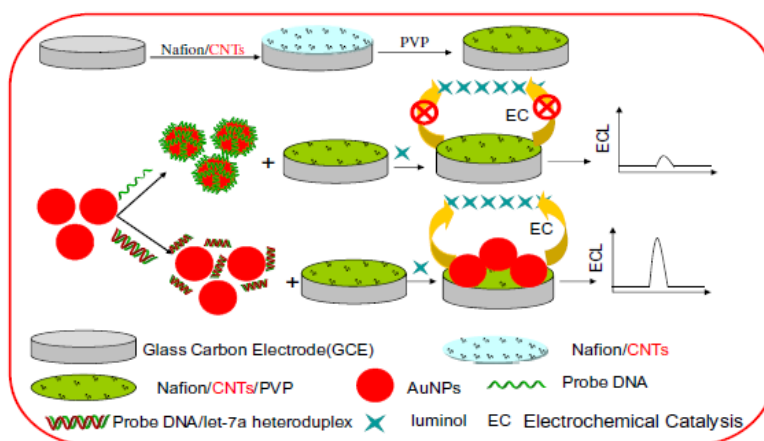
Figure 6. Schematic illustration of the sensing interface preparation process and possible mechanism of ECL reaction. Reprinted with permission from reference [23]. Copyright 2017 Springer Nature.

Au NCs are also non-toxic, biocompatible and stable. In an instance, a distance-dependent electrochemiluminescence resonance energy transfer (ERET) system was designed by Lei's group [22]. In this work, CdTe nanocrystals and Au NCs were used for signal output. The hairpin DNA-modified Au NCs were synthesized and conjugated to the carboxylated CdTe nanocrystals by amide coupling reaction. The ECL quenching of CdTe nanocrystals caused via the strong interaction between CdTe nanocrystals and Au NCs. The detection of miRNA was carried out with the aid of ligase. Long DNA-RNA heteroduplexes were formed when they were ligated by the selective ligase. So the ECL signal was recovered. According to the reporter, this distance-dependent ERET technology was utilized for the sequence-specific detection of miRNA. The method exhibits 6-order magnitude linear range. Very recently, a dual-wavelength ECL-RET ratiometric biosensor has been proposed to determine miRNAs in Xu's group (Figure 7) [33]. The Au NP-luminol-LDH donor and Au NC acceptor exhibited an ECL emission peak at 440 nm and 620 nm, respectively. In the presence of duplex-specific nuclease (DSN) and target miRNAs, the specific DNA/RNA binding and nuclease

cleaving facilitate the detachment of the captured Au NCs-DNA from the surface of Au NP luminol-LDH. This led to the increase in the ECL signal of Au NP-luminol-LDH and the decrease in fluorescence signal of Au NCs. The designed sensor allowed for quantitative detection of miRNAs in the concentration range of 10 aM ~ 100 pM. The detection limit was down to 9.4 aM. Besides plate and nanomaterials-modified electrodes, nanoporous membranes have also been widely employed in electric devices for designing of biosensors (Figure 8) [34]. Based on the nanopore ECL technology, Xu's group reported the ECL detection of miRNA by DSN-assisted target cycle. First, anodized aluminum oxide (AAO) was modified on ITO electrode to form nanopores, and Pt was coated to increase the conductivity of the electrode. The DNA-covered AuNPs were attached onto the AAO nanoporous membranes to weaken the ECL signal of luminol system or enhance the ECL signal of $Ru(bpy)_3^{2+}$ system. The DNA/miRNA hybrids on AuNPs surface can be cleaved by DSN to decompose the DNA and release miRNA for next hybridization cycle. Meanwhile, the decomposition of DNA made AuNPs removed from the membranes, thus resulting in the signal enhancement (luminol system) or decrease ($Ru(bpy)_3^{2+}$ system).
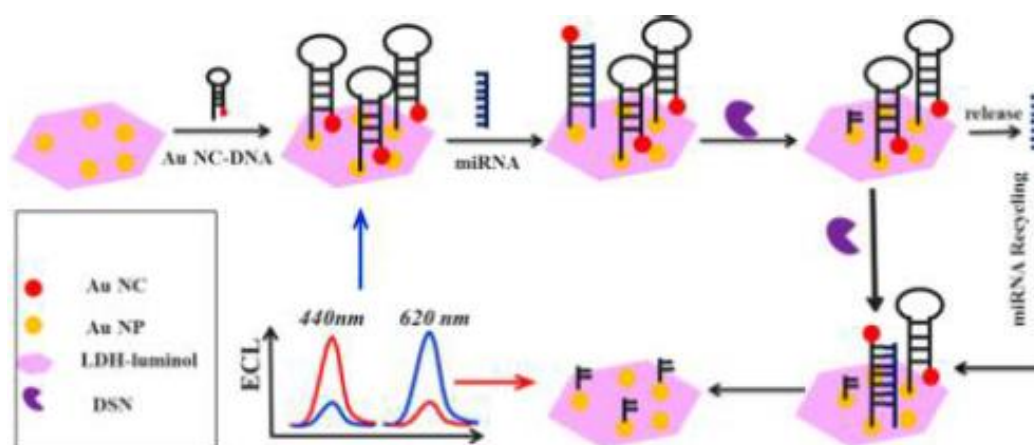
Figure 7. Schematic illustration of the dual-wavelength ratiometric ECL-RET biosensor for miRNA-107 detection. Reprinted with permission from reference [33]. Copyright 2018 American Chemical Society.
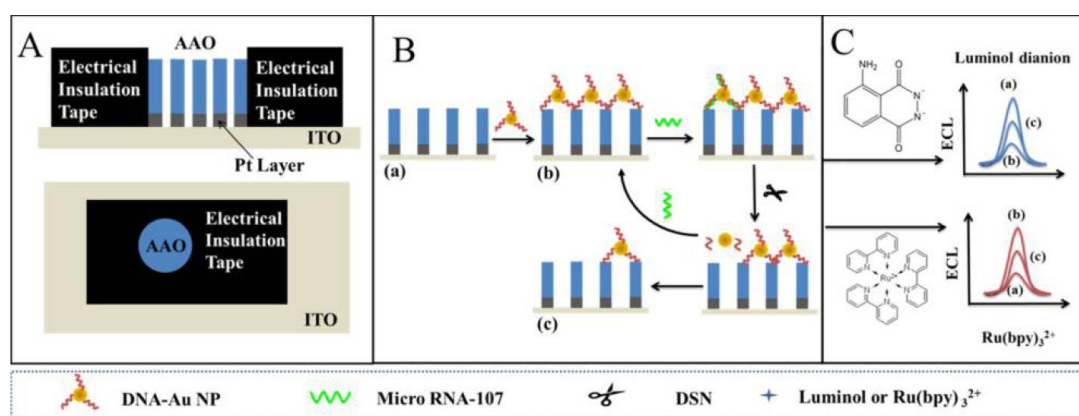
Figure 8. Schematic illustration of (A) construction of nanopore-based electrode, (B) preparation of nanopore-based ECL platform, and (C) ECL detection using luminol or $Ru(bpy)_3^{2+}$. Reprinted with permission from reference [34]. Copyright 2017 American Chemical Society.

2.3.3 Cu NCs

Cu NCs can be synthesized with DNA templates through the formation of stable A-Cu^{2+}-T bond. With Cu NCs as signal labels, Chai's group designed an ECL biosensor by the signal amplification of phi29 and Mn^{2+} DNAzyme-assisted target recycling and tetrahedral DNA nanostructures (TDN1, TDN2) [35]. As shown in Figure 9, binding of the inactive DNAzyme motor (DNA1) to the target miRNA-155 triggered the hybridization between the target and the locking strand (DNA2). Such strand-displacement reaction led to the formation of a DNA1/DNA3 duplex. In the presence of Mn^{2+}, the inactive DNAzyme was activated, driving DNA walker and cleaving DNA3 to release the target and a new DNA (Apt1). The Apt1 contains three segments: a short sequence P* (8AT), tandem periodic AT sequence, and ATP recognition sequence. ATP aptamer 2 (Apt2) is located on the top of TDN2-modified surface. The interaction between ATP and Apt1 as well as Apt2 made the P* sequence close to the P sequence of TDN1, thus facilitating the formation of the P/P* hybrid. In the presence of phi29 and deoxynucleotides, the P/P* hybrid induced the DNA polymerization to form AT-rich dsDNA. The dsDNA polymerization of Apt1 facilitated the detachment of Apt2 and ATP from Apt1. Apt2 and ATP were then removed on the sensor surface until the generation of all dsDNA. The AT-rich dsDNA acting as a ligand allowed for the electrochemical generation of Cu NCs on the vertex of TDN1 by the formation of A-Cu^{2+}-T bonds.
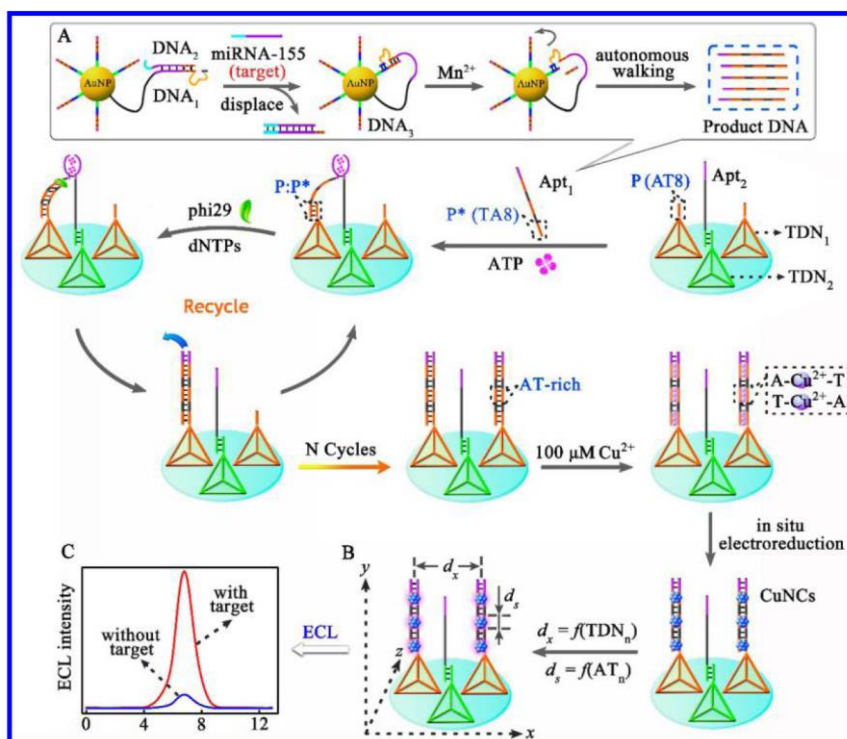
Figure 9. Schematic illustration of the nanocranes-based biosensor: (A) target-nucleotide transduction-amplification strategy; (B) programmable modulation of the ECL efficiency of Cu NCs; (C) signal comparison of miRNA-155 detection (dx = lateral spacing of Cu NCs; ds = particle size of Cu NCs). Reprinted with permission from reference [35]. Copyright 2018 American Chemical Society.

Therefore, the particle size and lateral spacing of Cu NCs were respectively tuned by the distribution of AT sequence and the fixed size of TDN. This improved the ECL emission of Cu NCs because of the higher loading capacity and lower collision loss. This method showed a wide linear range (100 aM ~ 100 pM) and a low detection limit (36 aM). At the same time, the group developed another ultrasensitive ECL biosensor for detecting miRNA-21 [36]. In the method, the in-situ generated Cu NCs acted as the luminophore and titanium dioxide (TiO_2) was employed as the coreaction accelerator. The produced AT-rich dsDNA reduced the aggregation-caused self-etching effect of Cu NCs, thus improving the emitting of Cu NCs. The introduced TiO_2 not only acted as the immobilizer of dsDNA-stabilized Cu NCs, but also played a role in accelerating the reduction of the coreaction reagent ($S_2O_8^{2-}$) for significantly enlarging the ECL efficiency of Cu NCs. The biosensor showed a good linear relationship in the range of 100 aM ~ 100 pM. The detection limit was found to be 19.05 aM.

2.3.4 Pt NPs

Pt NPs behaved similarly with Au NPs in some aspects for ECL. Chai and Yuan reported a method for the miRNA detection based on the dual miRNAs-fueled DNA nanogears in 2017 (Figure 10) [37]. Firstly, the nano-gear A consisted of different DNA strands of A1, A2, A3 and chain C was immobilized on the GCE electrode modified with CdS. The gear B was identical to that of A except that AuNPs modified on the B1 single strand. The single L1 modified with Pt NPs was hybridized with A1, B1, and the L2 single strand without any modifications hybridized with A2 and B2, they formed a stable hybrid structure. The ECL signal is quenched for the distance between AuNPs and CdS NCs. Subsequently, the target T1 bound to L1 and released L1, and the ECL signal is enhanced due to the distance increasing between AuNPs and CdS NCs. However, the target T2 could was combined with A3 and B3, resulted in the quenching of ECL signal again. This ECL signal off-on-off cycle mode could realize simultaneously detection of two kinds of miRNAs (miRNA21 and miRNA155).The detection limits were 0.16 fM and 0.33 fM, respectively.

With PtNPs as a co-reaction accelerator and O_2 as a co-reactant, a triple ECL system based on the rubrene as a luminophore was constructed for sensitive detection of miRNAs (Figure 11) [38]. First, the PtNFs were modified by the reduction reaction on rubrene micronods (RubMRs) to form PtNFs@RubMRs. Then, the single-stranded Fc-DNA modified with Fc was modified on the PtNFs@RubMRs, and the ECL signal is quenched due to the quenching effect of Fc. In the target-induced cyclic enzymatic amplification (TICEA) system, the target miRNA141 can hybridize with HPI-PtNPs. Under the action of the enzyme T1, the miRNA141 released by the hybridization chain continued to participate in the next cycle. S1/PtNPs not only replaced the Fc-DNA to restore the ECL signal, but also reacted with RubMRs to produce ROS. It caused the significantly enhancement of the ECL signal. This miRNA detection system has high sensitivity and low detection limit (2.1 aM).
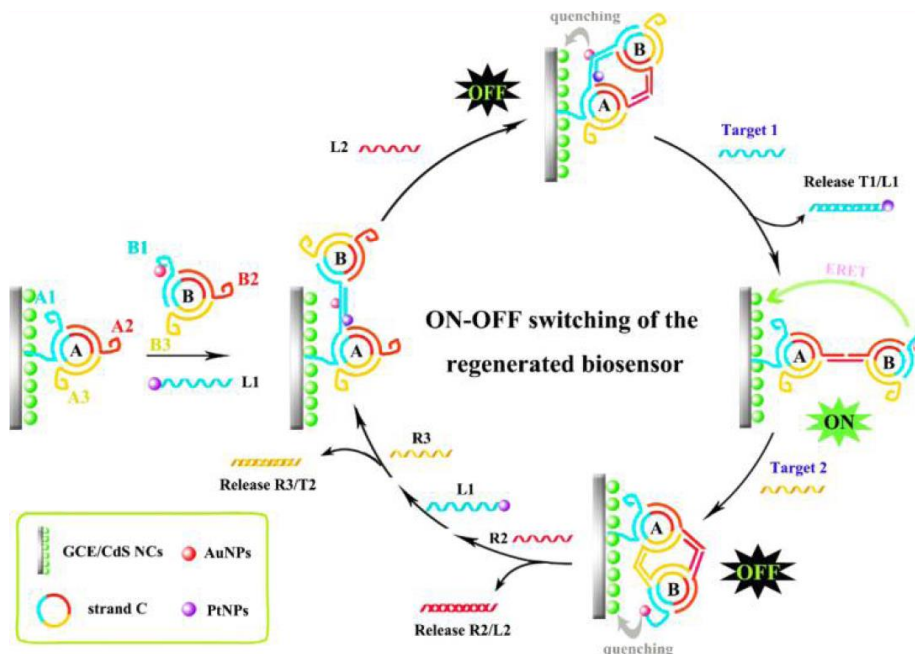
Figure 10. Operating principle of the dual miRNAs-fueled nanogear-based regenerated biosensor which realized the multiple ECL detection of miRNAs with single luminophore. Reprinted with permission from reference [37]. Copyright 2017 American Chemical Society.
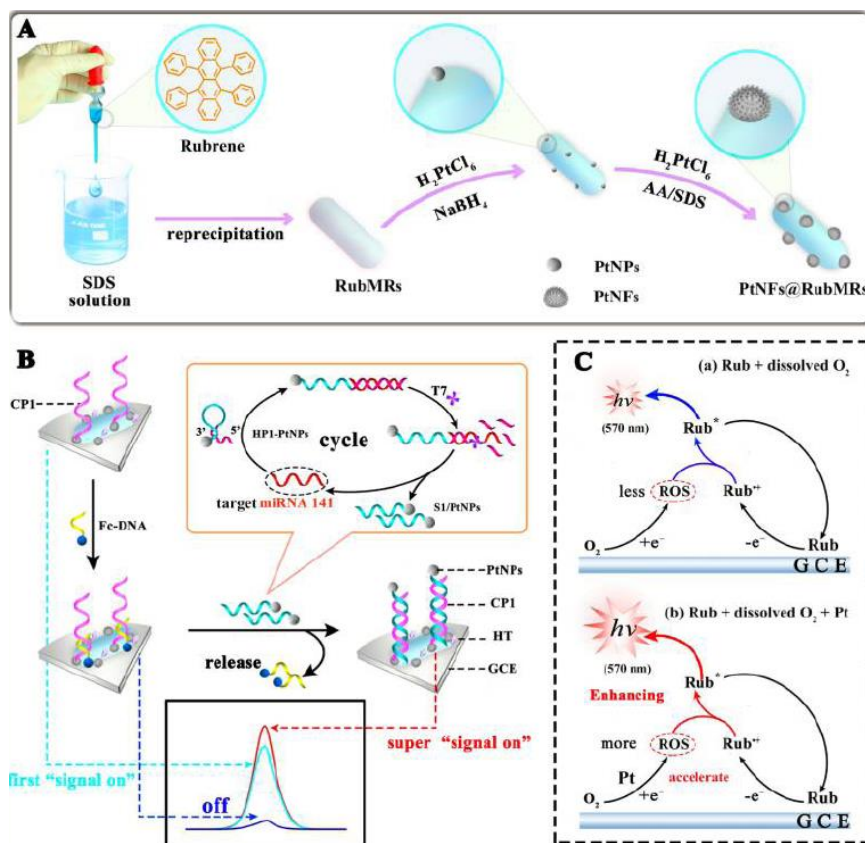
Figure 11. Operating principle of the dual miRNAs-fueled nanogear-based regenerated biosensor which realized the multiple ECL detection of miRNAs with single luminophore. Reprinted with permission from reference [38]. Copyright 2017 American Chemical Society.

In another newly paper published in 2018, diphenylen nanoparticles were used to immobilize Pt-Ag alloy particles to detect miRNAs [39]. The Pt-Ag@DPA NBs are modified on the GCE electrode. The swing-arm DNA probe (composed of DNA1 and DNA2) and the Fc-DNA were immobilized on the Pt-Ag alloy. ECL signal is weak due to a quenching effect of Fc. The target miNA141 hybridized with DNA1 to release DNA2, and the released DNA2 could hybridize with Fc-DNA. Under the action of enzyme T7, the hybrid of miRNA141 and DNA1 was cleaved to release the target miRNA141 for the next cycle. However, DNA2-Fc-DNA hybrid was also cleaved by the enzyme to release the Fc, and the naked DNA 2 continuously hybridized with the Fc-DNA on the surface of the electrode. With a large amount of Fc was released, the ECL signal was constantly enhanced. This method has high stability, good selectivity and low detection limit (29.5 aM).
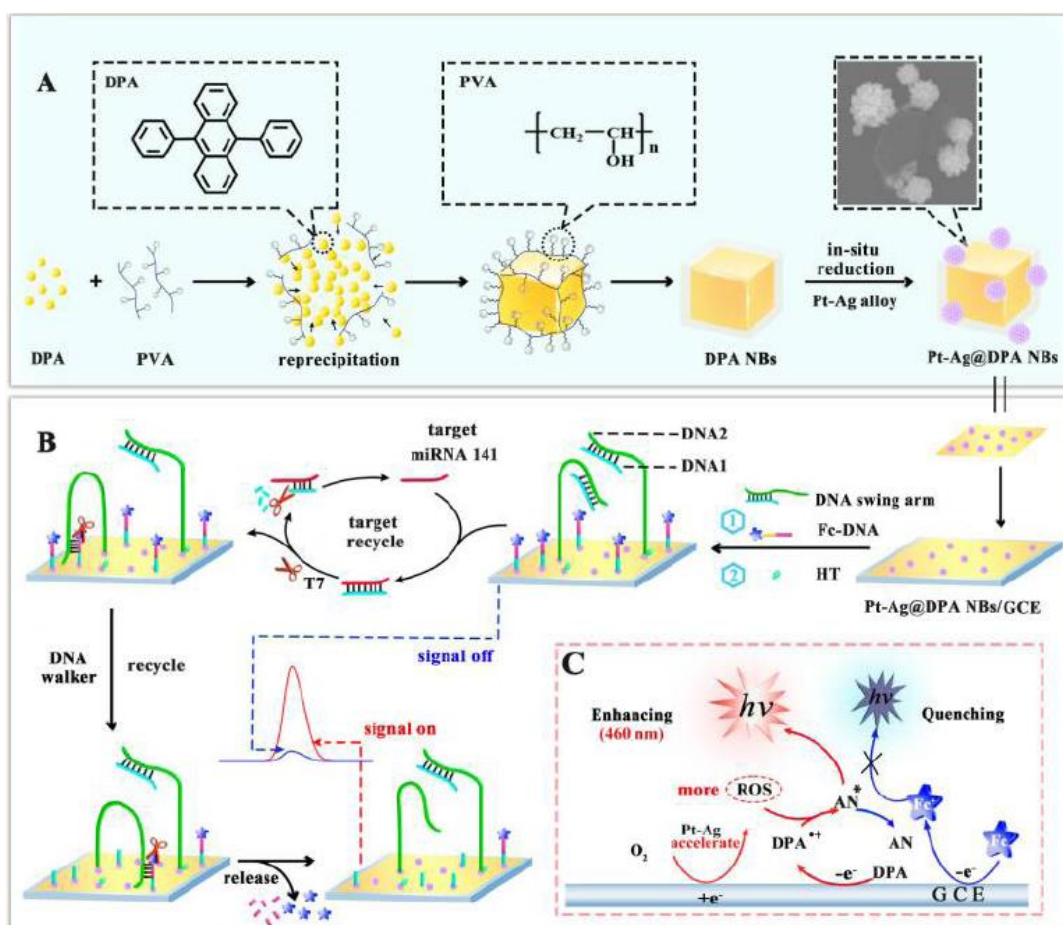
Figure 11. Schematic illustration of the preparation of Pt−Ag@DPA NBs (A), ultrasensitive detection of miRNA-141 based on the one-step DNA walker amplification (B), and the possible ECL mechanism of Pt−Ag@DPA NBs (C). Reprinted with permission from reference [39]. Copyright 2018 American Chemical Society.

2.4. Quantum dots

Quantum dots (QDs) are a group of novel materials widely used in electric devices for designing of biosensors [40, 41]. Chen's group have reported a method of the intercalation doxorubicin-conjugated QDs nanoparticles (Dox-QDs) into the DNA/RNA hybrids as the new signal

acquisition and amplification platform in 2015 [42]. A detection limit down to femtomolar level was obtained. According the report, the method was also coupled with acceptable selectivity in discriminating the target miRNA and against its family members as well as other interference sequence, thus being used to monitor miRNAs from human prostate carcinoma (22Rv1) cell lysates. Based on the QDs ECL technology, Lu et al. reported the method of ultrasensitive detection of miRNA by a dual amplification strategy with adriamycin-CdTe QDs [43]. Firstly, ssDNA1 is adsorbed on Fe_3O_4 magnetic beads. The target can be hybridized with ssDNA1. The target and DNA reporters were excised under the action of the double-strand specific nuclease (DSN); the ssDNA2 was immobilized on the bare gold electrode to hybridize with DNA reporters, and the probes H1 and H2 served as strand-grending linkers and DNA reporters, thereby extending the length of the hybrid strand. The pores formed by the hybrid strands can just wrap Dox-QDs (adriamycin-CdTe quantum dots), which in turn enhances the ECL signal. The detection limit of this method is 10 aM.

CdSe@ZnS QDs were used as receptor in some methods of detection of miRNA. For example, ECL-RET was used to detect miRNA-141 in an ultrasensitive manner in Li's group by combining donor and acceptor in a nanostructure to reduce energy loss (Figure 12) [44]. The method has a dual amplification strategy: target cycles and dual signal output conversion. Using $Ru(dcbpy)_3^{2+}$ as a donor and CdSe@ZnS QDs as a receptor, the capture probe 1 was immobilized on QDs-$Ru(dcbpy)_3^{2+}$ by amidation reaction to form the ECL nanolabels. The reporter DNA formed by the target cycle can be hybridized to the capture probe 2 immobilized on the GCE/Au electrode. After the signal probe was incubated with the GCE electrode, the probe 2 captured the signal probe. Finally, the ECL biosensor achieves quantitative detection of miRNA-141 by the change in the ratio of ECL response to miRNA-141 concentration.
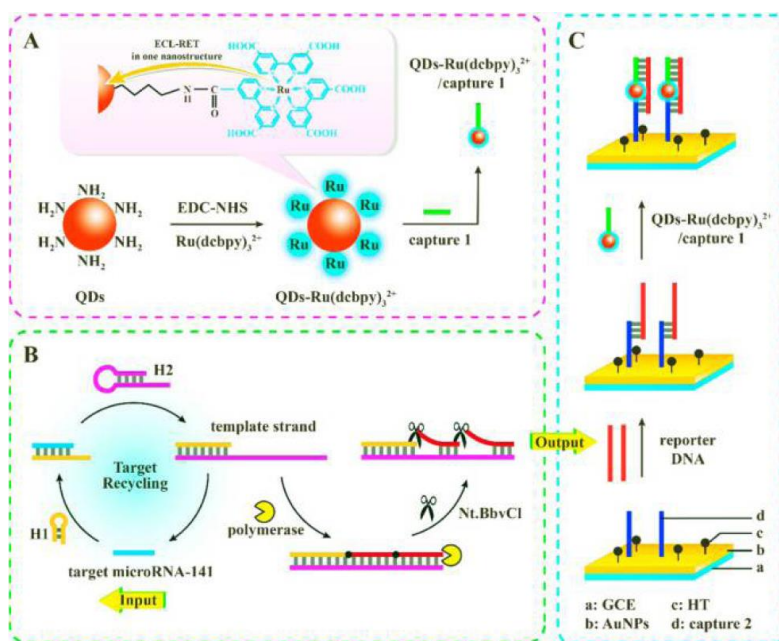
Figure 12. Construction of the miRNA biosensor based on the novel high-efficient ECL-RET in one nanostructure. Reprinted with permission from reference [44]. Copyright 2017 American Chemical Society.

In another paper, a regenerative sensor was fabricated by DNA nanomachine with dye AF488 as a donor and CdSe@ZnS as a receptor (Figure 13) [45]. The ultrasensitive detection of miRNA was realized by the principle of ECL-RET. A small amount of miRNA generated a large amount of reporter DNA through target circulation, and the reporter DNA was turned off by hybridization to open DNA tweezer. Meanwhile, AF488 and CdSe@ZnS QDs are close to each other, and the ECL signal was enhanced by the action of the ERET. In another protocol, target 1 (miRNA-141) was hybridized with probe DNA (pDNA) anchored on the CdS QDs-modified sensor surface [46]. The capture of trigger DNA (tDNA) by miRNA-141 induced the generation of a long ssDNA nanotail by the TdT-mediated DNA polymerization. Then, the resulting ssDNA can capture large numbers of Fc-peptide ssDNA conjugates by hybridization. The ECL intensity decreased greatly because of the efficient quenching effect of Fc to CdS QDs. This allowed for the ultrasensitive detection of miRNA-141 down to 33 aM. This method also allowed for the detection of target 2 (MMP-2) that can cleave the Fc-peptide-ssDNA conjugates. The cleavage caused the release of Fc tags from the sensor surface, thus leading to an enhancement in the ECL signal. As a result, MMP-2 can be determined with a detection limit of 33 fg/mL. The proposed sensor platform can be used to detect the biomarkers in both cancer cell and serum sample with satisfactory results.
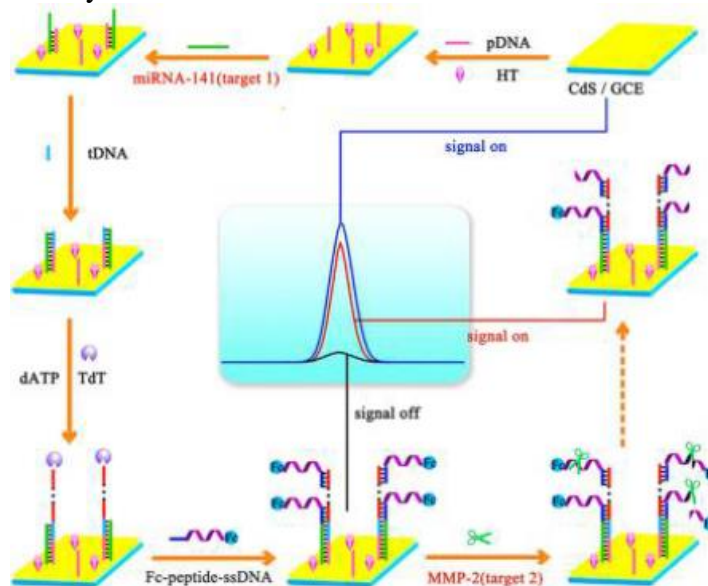
Figure 13. Fabrication of the ECL biosensing platform for the detection of multiple types of biomarkers on a single interface. Reprinted with permission from reference [46]. Copyright 2012 American Chemical Society.

Carbon quantum dots (CQDs) have attracted attentions due to their particular properties and functions, such as low toxicity, good biocompatibility, excellent light stability, and sturdy chemical inertness. In a recently published article, a miRNAs ECL biosensor based on the DNA-functionalized nitrogen-doped CQDs as the signal enhancers was reported [47]. In this work, the hairpin probe1-N-CQDs with assistant probe and miRNA formed a Y junction structure. Nicking enzymes Nb.BbvCI can cleave the junction structure to release miRNA and assistant probe. The released miRNA and

assistant probe then initiated the next recycling process. Furthermore, the produced N-CQDs-DNA hybridized with hairpin probe 2 attached on the GO/Au composite-modified electrode. This caused the enhancement in ECL intensity. Thus, the detection sensitivity of the method was improved by the signal amplification of target-induced cycling. The ECL intensity increased with the increase of miRNAs concentration in the range of 10 aM ~ 10^4 fM. The detection limit is down to 10 aM, facilitating its practical applications in clinical diagnosis.

Furthermore, Graphene QDs (GQDs) have also been used to develop a sensing platform to detect miRNA by dual signal amplification (Figure 14) [48]. First, the GQDs were immobilized on PTCA-NH$_2$ to increase the stability of GQDs. Then, Au@Fe$_3$O$_4$ immobilized with a large number of DNA probes was modified on PTCA-NH$_2$. Au can increase the rate of electron conduction, while Fe$_3$O$_4$ can achieve magnetic separation. The formed GQDs/PTCA−NH$_2$/Au@Fe$_3$O$_4$ material is immobilized on the surface of the GCE electrode, and the hairpin DNA probe (HP) is immobilized on the electrode by the Au-S bond. The helper DNA can simultaneously hybridized HP and the target miRNA. The T7 exonuclease can cleave the hybrid to release the miRNA and helper DNA to participate in the next cycle. Single-stranded DNA H1, H2, H3 and cross-linked DNA self-assemble to form Y-shaped nanostructures, and then the ECL signal is significantly enhanced by in situ reduction of AgNPs in the 3D DNA backbone due to electrostatic interaction. There are two major innovations in this design: (1) GQDs/PTCA−NH$_2$/Au@Fe$_3$O$_4$ nanomaterials are immobilized on the electrode surface due to the film-forming properties, which increases the stability and overcomes the water-soluble characteristics of GQDs, and (2) the effect of CEAM and AgNPs makes the method more sensitive. A type of boron-doped GQD (BGQD) with higher stability and lower impedance was synthesized in another work [49]. The BGQDs modified on the probe were close to the AuNPs modified on the Pt electrode when no target miRNA was added, and the ECL signal became stronger. But the probe structure was opened with the distance increased between them after the miRNA being added, and the ECL signal was weakened. So, the intensity of the ECL signal was related to the amount of miRNA.
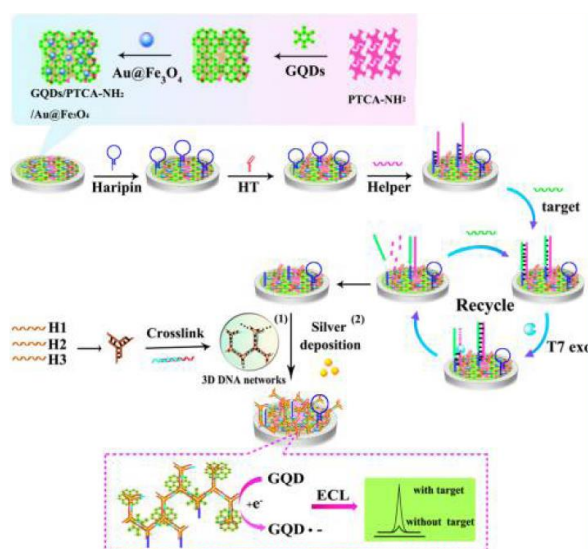
Figure 14. Designed illustration of the proposed biosensor and ECL reaction mechanism for sensitive detection of miRNA. Reprinted with permission from reference [48]. Copyright 2015 National Academy of Sciences.

MoS$_2$ QD acted as a type of novel nontoxic nanomaterial shows good ECL performance. Cao and coworkers reported the use of K$_2$S$_2$O$_8$ as a co-reactant to study the cathodic ECL behavior of MoS$_2$ QDs and to detect miRNA by adjusting the distance between MoS$_2$ quantum dots and Ag-PAMAM NCs [50]. When the distance between the two is very close, ECL quenching occurs due to electron resonance transfer. Conversely, when the distance between the two is relatively long, the ECL signal is enhanced due to the influence of surface plasmon resonance.

2.5. Carbon materials

Among numerous nanomaterials, graphene-based materials present many excellent properties such as large specific surface area, high electronic conductivity and outstanding biocompatibility. Graphene oxide (GO) has several kinds of function groups which can easily load plenty of antibodies, enzymes, DNAs, aptamers and various labels. It has been used for a dual signal amplification of ECL biosensors. For example, Based on gold nanopartical functionalized reduced graphene oxide (Au-rGO), the ECL signal is enhanced by the intramolecular reaction of PEI-Ru (II) and its intermolecular reaction with TSC (thiosemicarbazone) [51]. TSC can be used not only as an attachment to AuNPs, but also as an intermolecular reaction with PEI-Ru(II). This made the method ahead of others. In addition, the target can be recycled without the participation of enzymes. The high sensitivity and low detection limit were achieved. Moreover, a TAEA-PTCA@GO composite had been applied in a signal-off ECL biosensor for miRNA assay (Figure 15) [52]. First, a ternary "Y" structure for ECL signal quenching by ferrocene was established after the target miRNA triggered the phi29-mediated SDA with the assistant probe hybridization.
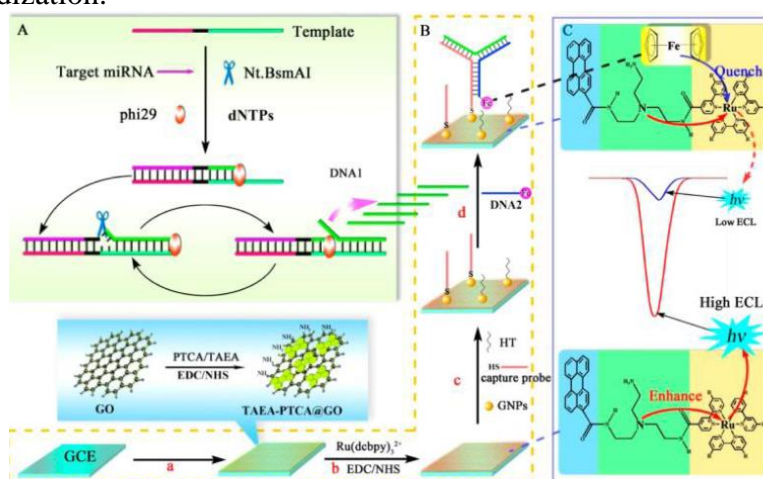
Figure 15. Schematic diagrams of the sensor: (A) the target induced cycling reaction based on the phi29-mediated SDA; (B) fabrication of the biosensor: (a) modifying GCE with TAEA-PTCA@GO composite, (b) cross-linking Ru(dcbpy)$_3^{2+}$, (c) assembly of GNPs, capture probe and HT, (d) the forming of "Y" structure; (C) the ECL enhancement mechanism of the self-enhanced Ru(II) composite and the ECL quenching by ferrocene along with the forming of "Y" structure. Reprinted with permission from reference [52]. Copyright 2015 Springer Nature.

Finally, the ECL intensity decreased with increasing concentration of the target miRNA. The sensitivity of biosensor was advanced based on the efficient signal amplification caused by the target induced cycling reaction. Besides this, a self-enhanced Ru(II) ECL system was designed in this report and demonstrated a stable and strong initial signal. Thus, the concentration range of ECL assay for miRNA-21 detection varied from 10 aM to 1.0 pM with a detection limit down to 3.3 aM.

GO was also utilized in another ultrasensitive faraday cage-type ECL assay for femtomolar miRNA-141 with hybridization chain reaction [53]. With the assisted cascade amplification, HCR combined with Faraday cage structure to construct a novel ECL sensor with a detection limit of 0.03 fM. The three highlights of the sensor were that (1) the hybridization chain formed by HCR carrying the Ru(phen)$_3^{2+}$ signal molecule to enhance the ECL signal, (2) the large surface area of GO could capture more HCR hybridization chains, and (3) the production of Outer Helmholtz Plane (OHP) allowed Ru(phen)$_3^{2+}$ on the signal unit to participate in the reaction, then significantly enhancing the ECL signal intensity. Afterwards, a faraday cage multi-function electrochemical sensor that enables ultra-sensitive detection of miRNAs was developed by Lu and coworkers [54]. Based on Fe$_3$O$_4$@Au MNPs-cDNA as the capture unit and (sDNA&luminol)@GO as the signal unit, the capture unit-miRNA-21-signal unit complex was formed in the presence of miRNA. Moreover, the large surface area of GO made it possible to load a large number of luminols, thus the ECL signal was enhanced furtherly. The high stability was the another advantage of the method.
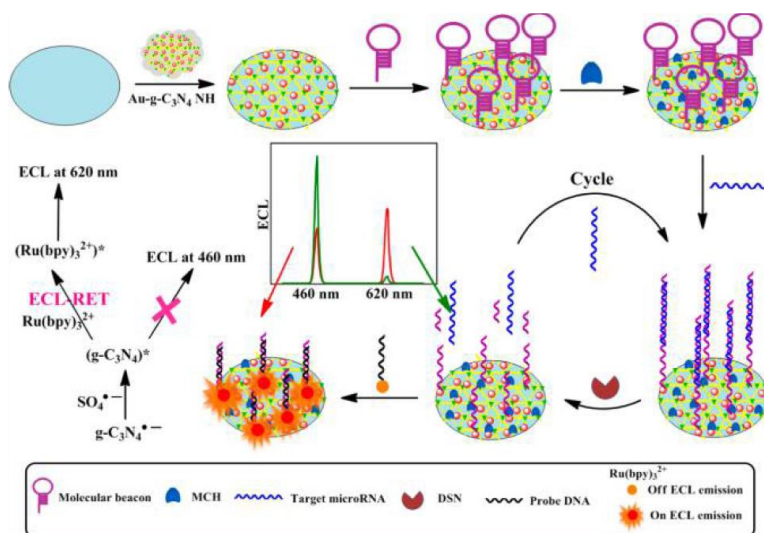
Figure 16. Schematic illustration of the dual-wavelength ratiometric ECL-RET biosensor configuration strategy. Reprinted with permission from reference [56]. Copyright 2016 American Chemical Society.

Recently, a newly strategy-ratiometric assay was particular, in which the quantification is dependent upon the ratio of two signals but not absolute values. This double-signal ratiometric method can greatly reduce the variation induced by the environmental change. Thus, the ratiometric measurement is more precise than the single-signal measurement [55]. For an instance, a dual-wavelength ECL ratiometry based on resonance energy transfer between Au nanoparticles functionalized g-C$_3$N$_4$ nanosheet and Ru(bpy)$_3^{2+}$ was reported for miRNA detection by Feng's group

(Figure 16) [56]. The g-C_3N_4 nanosheet modified with AuNPs was the donor and the $Ru(bpy)_3^{2+}$ was the acceptor. When they were close to each other, energy resonance transfer could occur and cause a change in the ECL signal. The strong ECL signal of Au-g-C_3N_4 was in 460 nm and the stronger signal of $Ru(bpy)_3^{2+}$ was at 620 nm. When ECL-RET occured, the ECL signal of Au-g-C_3N_4 at 460 nm was weakened while Ru $(bpy)_3^{2+}$ signal was enhanced. The same signal changes were observed at 620 nm. Therefore, the concentration of miRNA could be determined from the signal ratio ECL460 nm/ECL620 nm.

2.6. Metal organic framework

Metal organic frameworks (MOFs) are a class of porous coordination polymers with one-, two-, or three-dimensional structures. They can be made by the coordination of metal ions and organic ligands. Some of MOFs nanosheets exhibit large specific surface area and high conductivity, thus promoting their applications in electrochemical and electrochemiluminescent sensing devices. Liu and Ge have developed an ECL biosensor for miRNA-155 detection based on tris(bipyridine)ruthenium(II) functionalized MOF materials (RuMOF) and hairpin assembly target recycling (HTR) [57]. The capture probe H1 with hairpin structure modified onto the electrode by Au-S bond can capture the target miRNA-155 by hybridization, thus opening the hairpin structure of H1. The residual fragment of H1 is hybridized with the DNA probe H2 to release miRNA-155 due to the formation of a more stable H1-H2 structure. The residual fragment of H2 in the H1-H2 structure can hybridize with DNA-1 on the surface of RuMOFs. Addition of Hg^{2+} resulted in the release of $[Ru(bpy)_3]^{2+}$ from RuMOFs to produce an ECL signal. Without miRNA-155, the hairpin structure of H1 can not be opened. Consequently, probe H2 and RuMOFs can not be anchored on the electrode surface, and no ECL signal was observed. In this process, the released miRNA-155 can continue to participate in the next round of hybridization, thus amplifying the signal. Moreover, Guo's group developed a Faraday-cage electrochemical biosensor for miRNA-141 detection with RuMOFs as the reporters [58]. In this work, Fe_3O_4 nanoparticles coated with SiO_2 nanoparticles are modified with AuNPs. The nanocomposites ($Fe_3O_4@SiO_2@Au$) were used to immobilize the capture probe DNA. In the presence of miRNA-141, RuMOFs modified with signal probe DNA can be conjugated with $Fe_3O_4@SiO_2@Au$. The resulting products were captured by a magnetic GCE electrode. The Faraday-cage structure allows all molecules on the reporters to participate in the electrode reaction, thus producing a strong ECL signal.

4. CONCLUSION

As a highly sensitive analytical method, ELC has been used for miRNAs detection with satisfactory results. With the development of nanotechnology and portable devices, the combination of novel detection strategies, bipolar electrodes sensing platform and wireless transmission will make the ECL sensors more miniaturized and portable. In addition, ECL imaging analysis and high-throughput analysis will become popular based on the current investigations.

References

1. H. Dong, J. Lei, L. Ding, Y. Wen, H. Ju and X. Zhang, *Chem. Rev.*, 113 (2013) 6207.
2. J. Li, S. Tan, R. Kooger, C. Zhang and Y. Zhang, *Chem. Soc. Rev.*, 43 (2014) 506.
3. N. Xia, Y. J. Zhang, X. Wei, Y. P. Huang and L. Liu, *Aanl. Chim. Acta*, 878 (2015) 95.
4. L. Liu, Y. P. Gao, H. P. Liu and N. Xia, *Sensor. Actuat. B: Chem.*, 208 (2015) 137.
5. N. Xia, K. Liu, Y. Zhou, Y. Li and X. Yi, *Int. J. Nanomed.*, 12 (2017) 5013.
6. L. Liu, N. Xia, H. P. Liu, X. J. Kang, X. S. Liu, C. Xue and X. L. He, *Biosens. Bioelectron.*, 53 (2014) 399.
7. Y. Zhuo, H. Wang, Y. Lei, P. Zhang, J. Liu, Y. Chai and R. Yuan, *Analyst*, 143 (018) 3230.
8. N. Xia, X. Wang, B. Zhou, Y. Wu, W. Mao and L. Liu, *ACS Appl. Mater. Interfaces*, 8 (2016) 19303.
9. W. Shao, X. Sui and G. Wang, *Int. J. Electrochem. Sci.*, 12 (2017) 11506.
10. A. A. Jamali, M. Pourhassan-Moghaddam, J. E. N. Dolatabadi and Y. Omidi, *Trac-Trend. Anal. Chem.*, 55 (2014) 24.
11. B. N. Johnson and R. Mutharasan, *Analyst*, 139 (2014) 1576.
12. T. Kilic, A. Erdem, M. Ozsoz and S. Carrara, *Biosens. Bioelectron.*, 99 (2018) 525.
13. X. Zhao, W. Liu, B. Zhou, S. Liu and G. Han, *Int. J. Electrochem. Sci.*, 10 (2015) 8910.
14. P. Zhang, X. Wu, Y. Chai and R. Yuan, *Analyst*, 139 (2014) 2748.
15. X. Li, A. Chen, Y. Chai and R. Yuan, 142 (2017) 2185.
16. L. Lu, C. Liu, T. Kang, X. Wang, G. Guo and W. Miao, *Sensor. Actuat. B: Chem.*, 255 (2018) 35.
17. J. Jiang, Q. Li, W. Wang, X. Chen and Z. Chen, *Int. J. Electrochem. Sci.*, 13 (2018) 587.
18. T. Liu, X. Chen, C.-Y. Hong, X.-P. Xu and H.-H. Yang, *Microchim. Acta*, 181 (2014) 731.
19. C. Liu, L. Wang, L. Lu and T. Kang, *Anal. Methods*, 9 (2017) 6760.
20. Y. Wang, S. Y. Ji, H. Y. Xu, W. Zhao, J. J. Xu and H. Y. Chen, *Anal. Chem.*, 90 (2018) 3570.
21. M. Wang, Y. Zhou, H. Yin, W. Jiang, H. Wang and S. Ai, *Biosens. Bioelectron.*, 107 (2018) 34.
22. Y. Cheng, J. Lei, Y. Chen and H. Ju, *Biosens. Bioelectron.*, 51 (2014) 431.
23. H. Xiong and X. Zheng, *Microchim. Acta*, 184 (2017) 1781.
24. N. Xia, X. Wang, J. Yu, Y. Wu, S. Cheng, Y. Xing and L. Liu, *Sensor. Actuat. B: Chem.*, 239 (2017) 834.
25. N. Xia, L. Liu, Y. Chang, Y. Hao and X. Wang, *Electrochem. Commun.*, 74 (2017) 28.
26. Y. Y. Zhang, Q. M. Feng, J. J. Xu and H. Y. Chen, *ACS Appl. Mater. Interfaces*, 7 (2015) 26307.
27. A. Chen, S. Ma, Y. Zhuo, Y. Chai and R. Yuan, *Anal. Chem.*, 88 (2016) 3203.
28. D. Deng, L. Liu, Y. Bu, X. Liu, X. Wang and B. Zhang, *Sensor. Actuat. B: Chem.*, 269 (2018) 189.
29. L. Liu, D. Deng, Y. Wang, K. Song, Z. Shang, Q. Wang, N. Xia and B. Zhang, *Sensor. Actuat. B: Chem.*, 266 (2018) 246.
30. L. Peng, P. Zhang, Y. Chai and R. Yuan, *Anal. Chem.*, 89 (2017) 5036.
31. Z. Xu, L. Liao, Y. Chai, H. Wang and R. Yuan, *Anal. Chem.*, 89 (2017) 8282.
32. Y. Qiao, Y. Li, W. Fu, Z. Guo and X. Zheng, *Anal. Chem.*, 90 (2018) 9629.
33. X. L. Huo, N. Zhang, H. Yang, J. J. Xu and H. Y. Chen, *Anal. Chem.*, 90 (2018) 13723.
34. X. L. Huo, H. Yang, W. Zhao, J. J. Xu and H. Y. Chen, *ACS Appl. Mater. Interfaces*, 9 (2017) 33360.
35. Y. Zhou, H. Wang, H. Zhang, Y. Chai and R. Yuan, *Anal. Chem.*, 90 (2018) 3543.
36. H. Liao, Y. Zhou, Y. Chai and R. Yuan, *Biosens. Bioelectron.*, 114 (2018) 10.

37. P. Zhang, Z. Lin, Y. Zhuo, R. Yuan and Y. Chai, *Anal. Chem.*, 89 (2017) 1338.
38. J. L. Liu, Z. L. Tang, Y. Zhuo, Y. Q. Chai and R. Yuan, *Anal. Chem.*, 89 (2017) 9108.
39. J.-L. Liu, Z. L. Tang, J. Q. Zhang, Y. Q. Chai, Y. Zhuo and R. Yuan, *Anal. Chem.*, 90 (2018) 5298.
40. J. J. Shi, Q. Q. Zhang, W. Hu and P. Yang, *Int. J. Electrochem. Sci.*, 13 (2018) 3575.
41. N. Xia, B. Zhou, N. Huang, M. Jiang, J. Zhang and L. Liu, *Biosens. Bioelectron.*, 85 (2016) 625.
42. Y. Chen, Y. Xiang, R. Yuan and Y. Chai, *Anal. Chim. Acta*, 891 (2015) 130.
43. L. Lu, B. Yang and T. Kang, *Appl. Surf. Sci.*, 426 (2017) 597.
44. Z. Li, Z. Lin, X. Wu, H. Chen, Y. Chai and R. Yuan, *Anal. Chem.*, 89 (2017) 6029.
45. P. Zhang, Z. Li, H. Wang, Y. Zhuo, R. Yuan and Y. Chai, *Nanoscale*, 9 (2017) 2310.
46. Y. Nie, P. Zhang, H. Wang, Y. Zhuo, Chai, Y. and R. Yuan, *Anal. Chem*, 89 (2017) 12821.
47. Q. Liu, C. Ma, X. P. Liu, Y. P. Wei, C. J. Mao and J. J. Zhu, *Biosens. Bioelectron.*, 92 (2017) 273.
48. P. Zhang, Y. Zhuo, Y. Chang, R. Yuan and Y. Chai, *Anal. Chem.*, 87 (2015) 10385.
49. T. Zhang, H. Zhao, G. Fan, Y. Li, L. Li and X. Quan, *Electrochim. Acta*, 190 (2016) 1150.
50. J.-T. Cao, F.-R. Liu, F. Hou, J. Peng, S.-W. Ren and Y.-M. Liu, *Analyst*, 143 (2018) 3702.
51. Y. Q. Yu, J. P. Wang, M. Zhao, L. R. Hong, Y. Q. Chai, R. Yuan and Y. Zhuo, *Biosens. Bioelectron.*, 77 (2016) 442.
52. A. Chen, G. Gui, Y. Zhuo, Y. Chai, Y. Xiang and R. Yuan, *Anal. Chem.*, 87 (2015) 6328.
53. J. Lu, L. Wu, Y. Hu, S. Wang and Z. Guo, *Biosens. Bioelectron.*, 109 (2018) 13.
54. J. Lu, L. Wu, Y. Hu, S. Wang and Z. Guo, *J. Electrochem. Soc.*, 164 (2017) B421.
55. H. Shao, H. Lin, J. Lu, Y. Hu, S. Wang, Y. Huang and Z. Guo, *Biosens. Bioelectron.*, 118 (2018) 247.
56. Q. M. Feng, Y. Z. Shen, M. X. Li, Z. L. Zhang, W. Zhao, J. J. Xu and H. Y. Chen, *Anal. Chem.*, 88 (2016) 937.
57. Y. Jian, H. Wang, F. Lan, L. Liang, N. Ren, H. Liu, S. Ge and J. Yu, *Microchim. Acta*, 185 (2018) 133.
58. H. Shao, J. Lu, Q. Zhang, Y. Hu, S. Wang and Z. Guo, *Sensor. Actuat. B: Chem.*, 268 (2018) 39.